http://dx.doi.org/10.5012/bkcs.2013.34.4.1137

Evaluating the Catalytic Effects of Carbon Materials on the Photocatalytic Reduction and Oxidation Reactions of TiO_2

Gulzar Khan, Young Kwang Kim, Sung Kyu Choi, Dong Suk Han,† Ahmed Abdel-Wahab,† and Hyunwoong Park‡,*

Department of Physics, Kyungpook National University, Daegu 702-701, Korea
†Chemical Engineering Program, Texas A&M University at Qatar, Education City, Doha, P.O. Box 23874, Qatar
*‡School of Energy Engineering, Kyungpook National University, Daegu 702-701, Korea. *E-mail: hwp@knu.ac.kr*
Received October 30, 2012, Accepted January 21, 2013

TiO_2 composites with seven different carbon materials (activated carbons, graphite, carbon fibers, single-walled carbon nanotubes, multi-walled carbon nanotubes, graphene oxides, and reduced graphene oxides) that are virgin or treated with nitric acid are prepared through an evaporation method. The photocatalytic activities of the as-prepared samples are evaluated in terms of H_2 production from aqueous methanol solution (photocatalytic reduction: PCR) and degradation of aqueous pollutants (phenol, methylene blue, and rhodamine B) (photocatalytic oxidation: PCO) under AM 1.5-light irradiation. Despite varying effects depending on the kinds of carbon materials and their surface treatment, composites typically show enhanced PCR activity with maximum 50 times higher H_2 production as compared to bare TiO_2. Conversely, the carbon-induced synergy effects on PCO activities are insignificant for all three substrates. Colorimetric quantification of hydroxyl radicals supports the absence of carbon effects. However, platinum deposition on the binary composites displays the enhanced effect on both PCR and PCO reactions. These differing effects of carbon materials on PCR and PCO reactions of TiO_2 are discussed in terms of physicochemical properties of carbon materials, coupling states of TiO_2/carbon composites, interfacial charge transfers. Various surface characterizations of composites (UV-Vis diffuse reflectance, SEM, FTIR, surface area, electrical conductivity, and photoluminescence) are performed to gain insight on their photocatalytic redox behaviors.

Key Words : Electrocatalyst, Charge separation, Water splitting, Solar, Artificial photosynthesis

Introduction

TiO_2 photocatalysis has been extensively studied in terms of hydrogen production from water and remediation of environmental pollutants.[1-4] Despite its several advantages, TiO_2 suffers from the unavailability of solar visible light due to a wide bandgap of *ca.* 3.2 eV and the fast charge recombination. Various approaches to overcome such limitations have been attempted including doping,[5-7] sensitization,[8-10] and surface modifications.[11,12] Among the surface modifiers, carbon materials appear to play multiple and unique roles in TiO_2 photocatalysis.[13-16] Carbon materials are diverse from traditional activated carbons (AC) and graphite (GP), one-dimensional graphitic carbon nanofibers (CNF), single- and multi-walled carbon nanotubes (SWNT and MWNT, respectively), and even to graphite oxides (GO) and reduced graphene oxides (RGO). Due to their large surface areas (max. > 1000 m^2/g), porosity, and electrical conductivity, they can increase the binding capability, change photocatalytic mechanism, and boost photocatalytic redox reactions such as H_2 production from water and remediation of environmental pollutants.

It has been reported that carbon materials induce synergy effects of photocatalytic H_2 production as well as photocurrent generations mostly due to their high electroconductivity. Zhang *et al.* reported that the photoelectrochemical performance of TiO_2 electrode is approximately five-fold enhanced by coupling with graphite-carbon.[17] MWNT[18-22] and SWNT[23-25] also have been consistently shown to increase photocatalytic H_2 production and photocurrent generation to varying degrees depending on preparation methods and carbon/TiO_2 ratios. Very recently, GO[26] and RGO[27-34] have received enormous attention as co-catalysts for TiO_2 photoelectrocatalytic reduction reactions. Their roles and effects are very similar to those of GP, MWNT, and SWNT in terms of electron sink and enhanced charge separation.

In contrast to the photocatalytic reduction (PCR) reactions, carbon effects on photocatalytic oxidation (PCO) reactions of TiO_2 appear to be more complicated and in some cases rather controversial. Colon *et al.*[35] and El-Sheikh *et al.*[36] reported the similar result that AC enhanced the PCO of phenol, whereas Torimoto *et al.*[37] and Yu *et al.*[38] found negative effects on the PCO of dichloromethane and azo dye, respectively. In the case of MWNT, counter effects for phenol[39,40] were observed as well due to different experimental conditions,[41] while the synergy between TiO_2 and SWNT for PCO reaction was not always positive.[42-44] CNF enhanced the PCO of gaseous acetaldehyde[45] but GP retarded the PCO of chlorophenoxyacetic acid.[46] RGO was reported to be highly effective in the PCO of methylene blue[47] while its role is intrinsically same as CNT[48] and its photostability is in question.[49]

The aim of this study is to evaluate the photocatalytic redox reactions of TiO_2/carbon materials and compare the

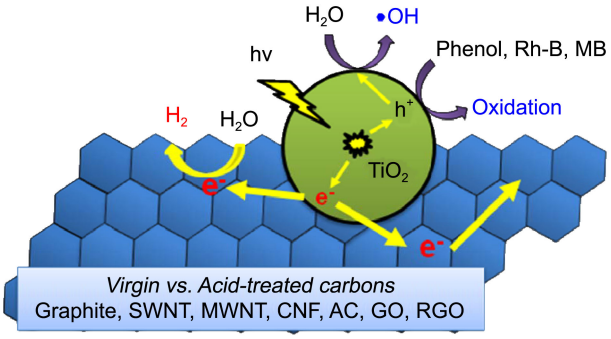

Scheme 1. Schematic illustration for photocatalytic redox reactions of TiO_2 and carbon composites.

effects of carbon materials. There are several articles which compare the photocatalytic effects (only PCO or PCR) between two different carbon materials (AC *vs*. carbon black,[50] AC *vs*. MWNT,[38] C60 *vs*. MWNT,[51] SWNT *vs*. MWNT,[44] and MWNT *vs*. RGO[33,47,48,52]). To the best of our knowledge, however, there are few reports on the systematic studies for the effects of carbon materials on the TiO_2 photocatalysis. Taking into account that carbon materials are expected to receive increasing attention, such comparison are highly necessary. For this, we attempted to evaluate the PCR and PCO activities of hybrid TiO_2 with seven different carbon materials (AC, CNF, GP, MWNT, SWNT, GO, and RGO) that were either virgin or acid-treated in terms of H_2 production from water and degradation of three model substrates (phenol, methylene blue, and rhodamine B) (Scheme 1). Surface characterizations (UV-Vis diffuse reflectance, SEM, BET surface area, electrical conductivity, and photoluminescence) were also performed.

Experimetal

Carbon Materials. Graphite (< 20 μm, Sigma), multi-walled carbon nanotubes (CM-100, Hanwha Nanotech), single-walled carbon nanotubes (ASA-100F, Hanwha Nanotech), carbon nanofibers (CNF-LSA, Carbon Nano Material Technology), and activated carbons (Alfa Aesar) were used as-received or after acid treatment. Graphite oxides and reduced graphene oxides were prepared by following a modified version of Hummer's method (Supporting Information).[53] For acid treatment the carbon materials were treated in a reflux system with nitric acid (1 M) for 1 h to change their physicochemical properties (see Table 1). Then, they were filtered with 0.45-μm PTFE filters (Millipore), washed with distilled water, and dried overnight at 80 °C.

Preparation of TiO_2/Carbon Binary and TiO_2/Carbon/Pt Ternary Composites. TiO_2/carbon binary composites were prepared by a simple evaporation method. First, approximately 10 mg of each carbon material (virgin or acid-treated) was dispersed in water in a 200-mL beaker and sonicated for 20 min. Commercial TiO_2 powder (Degussa P25; anatase and rutile mixture (8:2) with BET area of *ca.* 50 m^2/g) was added to the suspension at a ratio of 20:1 (TiO_2: carbon by weight) during sonication. Then, the mixed suspension was heated to 80 °C on a stir plate with air flowing across the surface of the suspension to accelerate the evaporation of water. After the water evaporated, the composite was dried overnight in an oven at 104 °C to avoid any physicochemical change of the carbon materials that occurs at higher temperatures in the presence of oxygen. In order to examine the effect of platinum, Pt was photodeposited on TiO_2/MWNT (TiO_2/MWNT/Pt), or on bare TiO_2 subsequently to which MWNT was coupled (TiO_2/Pt/MWNT). UV light was irradiated to the aqueous suspension of TiO_2 or TiO_2/MWNT with methanol (1 M) and chloroplatinic acid (H_2PtCl_6) for 30 min using a 200-W mercury lamp. The amount of platinum was fixed at 0.5 wt % with respect to TiO_2.

Table 1. Comparison of carbon materials for their physicochemical properties

Samples		Surface Area (m^3/g)	Electrical Conductivity (S/m)
AC	Virgin	851	1.70×10^{-1}
	Treated[a]	950	–
CNF	Virgin	130	2.87×10^{1}
	Treated	140	–
MWNT	Virgin	22	1.87×10^{3}
	Treated	178	1.42×10^{5}
SWNT	Virgin	100	2.93×10^{2}
	Treated	134	4.30×10^{4}
GP	Virgin	14	1.81×10^{4}
	Treated	9	1.46×10^{6}
GO	–	–	1.65×10^{0}
RGO	–	23	1.01×10^{3}

[a]Carbon samples were suspended in an aqueous mixture of 1 M HNO_3 for 1 h and recovered after washing with distilled water and drying at 80 °C.

Photocatalysis. The PCR activity of the composites was evaluated with H_2 production from aqueous methanol solution. For this, an aqueous suspension (25 mL) containing TiO_2/carbon sample (0.5 g/L) and methanol (10 vol %) was stirred in a Pyrex-glass reactor (*ca*. 39 mL volume) equipped with a quartz disc for light penetration. Prior to irradiation, nitrogen gas was purged through the suspension for 30 min. A solar simulator equipped with AM 1.5 G filter (LS-150 Xe, Abet Technologies) was used as a light source. To avoid thermal effects, the reactor was cooled to room temperature with an air cooler fan. During irradiation, the headspace gas (14 mL) of the reactor was intermittently sampled (100 uL) and analyzed for H_2 using a gas chromatograph (Young Lin, ACME 6100) equipped with a thermal conductivity detector and a carboxen 1000 packed column.

The PCO activity of the composites was also examined for remediation of aqueous phenol (PhOH), methylene blue (MB), and Rhodamine B (Rh-B). In each test, 12.5 mg of the composite was dispersed in substrate solutions of 25 mL ($[PhOH]_0$ = 0.5 mM; $[MB]_0$ = 0.1 mM; $[Rh\text{-}B]_0$ = 0.2 mM). To allow the adsorption equilibriums of substrates on the composites, the suspensions were stirred for 30 min in the

dark. Then the suspension was irradiated with the AM 1.5 light. Samples were taken every 15 min and the concentrations of phenol and byproducts were determined using a high performance liquid chromatography (HPLC, YL9100) equipped with a C18 column (Thermo). The HPLC eluent was composed of 55 vol % distilled water (0.1 vol % phosphoric acid included) and 45 vol% acetonitrile at a flow rate of 1 mL/min. The concentrations of MB and Rh-B were determined by recording their respective main absorption bands at 664 nm and 554 nm using a UV-Vis spectrophotometer (T60, GP Instrument). For examining OH radical generation, the photocatalytic decay of RNO (*N,N*-dimethyl-*p*-nitrosoaniline) was monitored by recording its absorption band at 440 nm.[54]

Surface Analysis. UV-Vis diffuse reflectance spectra (DRS) were obtained by using a UV-Vis spectrometer (UV-2450, Shimadzu). $BaSO_4$ was used as a reflectance standard. Scanning electron microscopy (SEM) measurements were performed using a field emission scanning electron microscope (Hitachi, S-4800) at an operating voltage of 3 kV. The Fourier transform infrared spectra (FTIR) of the samples were conducted on Spectrum GX and autoimage (PerkinElmer) using KBr for sample preparation. Photoluminescence spectra were recorded at room temperature using a spectrometer (f = 0.5 m, Acton Research Co., Spectrograph 500i, U.S.A.) equipped with an intensified photodiode array detector (Princeton Instrument Co., IRY1024, U.S.A.). A He-Cd laser (Kimmon, 1 K, Japan) with a wavelength of 325 nm and power of 50 mW was utilized as the excitation light source.

Results and Discussion

Photocatalytic H_2 Production. Figure 1 shows the photocatalytic H_2 production in AM 1.5 light-irradiated TiO_2/carbon suspensions with methanol (10 vol %) as an electron donor. It is surprising that TiO_2/carbon composites prepared simply *via* the evaporation processes are superior to bare TiO_2 in the photocatalytic H_2 production (Fig. 1(a)). In particular, TiO_2 composites with SWNT and MWNT exhibit the enhanced H_2 amounts by a factor of *ca.* 17 and 12, respectively, as compared to bare TiO_2 (Fig. 1(c)). However, physical mixings of TiO_2 and CNTs (TiO_2 + CNTs) reduce the H_2 generation likely due to loose interparticle interaction; nevertheless, their photocatalytic activities are still much higher than that of bare TiO_2. This indicates that the evaporation method is effective in coupling pre-crystallized TiO_2 (Degussa P25) and carbon materials, thereby allowing a facile charge transfer between them (see Fig. 2). TiO_2 composites with RGO, GO, CNF and AC also exhibit similar synergy effects for H_2 production by a factor of 3-5, whereas no H_2 was produced in TiO_2/GP.

Acid-treated carbon (a-carbon) materials were examined for their effects on the H_2 production as well. For this treatment, carbon materials were refluxed in 1 M HNO_3 for 1 h and recovered after drying at 80 °C. It is found that the effect of acid treatment largely varies depending on the kind of carbon materials. For example, H_2 production was enhanced by a factor of 4 with a-MWNT compared to virgin MWNT, while non-active virgin GP became highly active by acid treatment (Fig. 1(b) & (c)). Conversely, a-SWNT displayed reduced H_2 production and no H_2 was produced with a-AC and a-CNF.

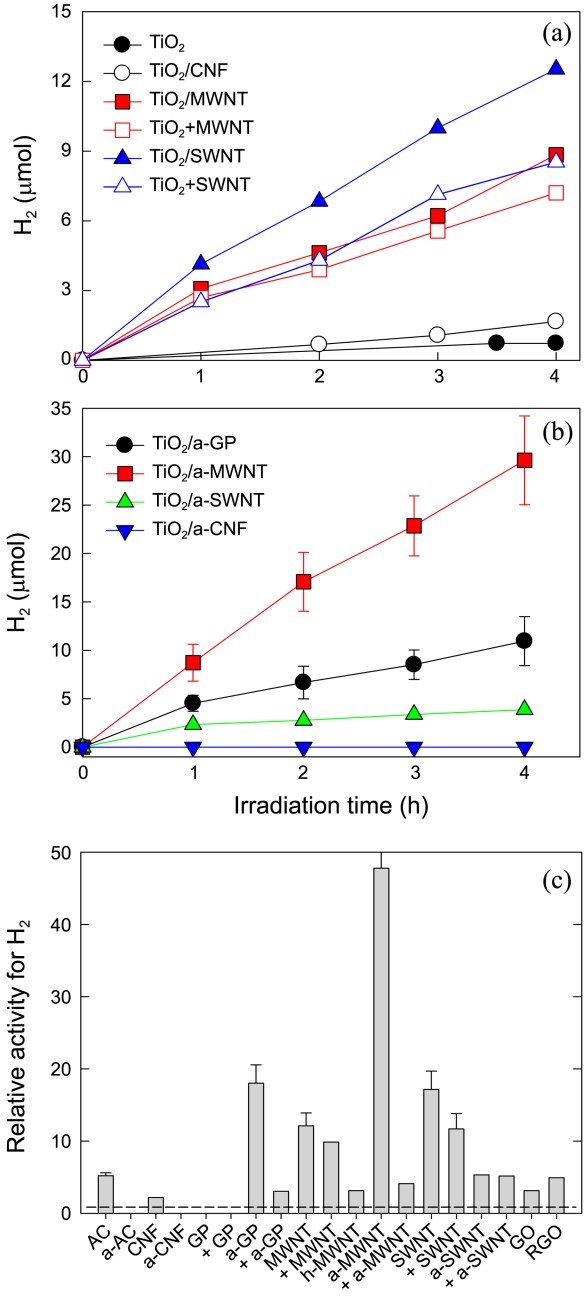

Figure 1. Time-profiled H_2 production in AM 1.5 light-irradiated suspensions of TiO_2 composites with (a) virgin carbon materials (b) acid-treated carbon materials. (c) shows the relative activity of TiO_2 composites with respect to bare TiO_2 in terms of H_2 production. "a" and "+" refer to acid treatment of carbon materials and physical mixing between TiO_2 and carbon, respectively. [catalyst] = 0.5 g/L; $[MeOH]_0$ = 10 vol %; N_2-purged for 30 min prior to photocatalysis. AC: activated carbon, CNF: carbon nanofiber, GP: graphite, MWNT: multi-walled carbon nanotubes, SWNT: single-walled carbon nanotubes, GO: graphite oxides, RGO: reduced graphene oxides.

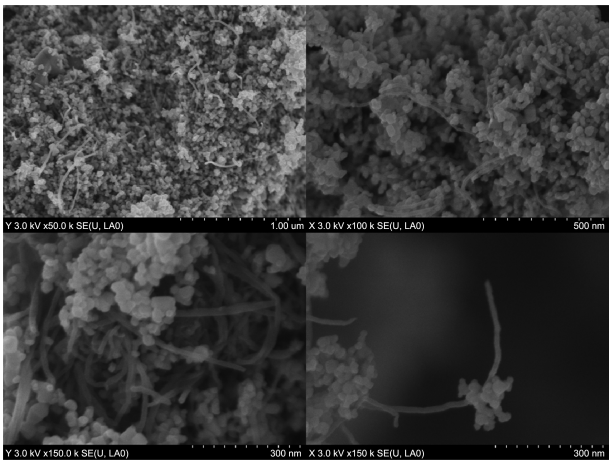

Figure 2. Scanning electron microscopic (SEM) images of TiO_2/a-MWNT.

In order to investigate the reasons for the different activities among carbon materials and activity changes by their acid treatment, surface characterization of TiO_2 composites were performed. Figure 3 shows the UV-Vis diffuse reflectance spectra of TiO_2/carbon composites. All the composites exhibited similar optical behaviors with bare TiO_2 in terms of onset wavelength (*ca.* 390 nm). Gradual increases of absorbance in visible light region (λ > 400 nm) may be ascribed to intrinsic property of carbon materials (Fig. S1) and the slight differences of absorbance among the composites are likely due to inhomogeneous mixing between TiO_2 and carbon materials. In a few cases, TiO_2/MWNT[55,56] generated H_2 under visible light likely due to formation of Ti-O-C bond just like carbon-doped TiO_2.[7]

If the optical property is not the main factor for enhanced H_2 production, facilitated electron transfer may be the alternative. To examine this conjecture, photoluminescence (PL) emission spectra for TiO_2 composites were obtained. As shown in Figure 4, bare TiO_2 exhibits a strong PL emission band at *ca.* 530 nm due to electron-hole recombination.[26,57] However, the PL emission bands of TiO_2 composites with MWNT, SWNT, and GP significantly decrease yet with

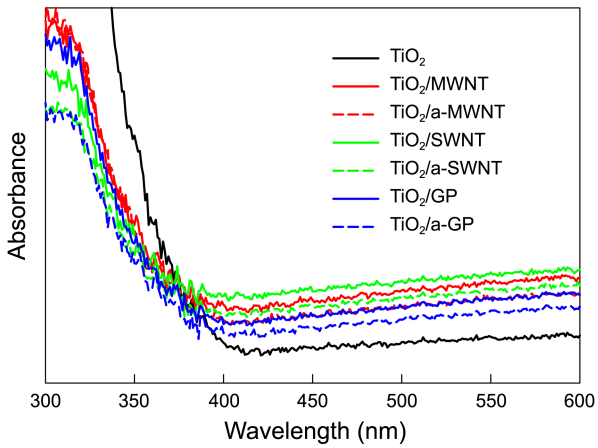

Figure 3. UV-Vis diffuse reflectance spectra of bare TiO_2 and TiO_2 composites.

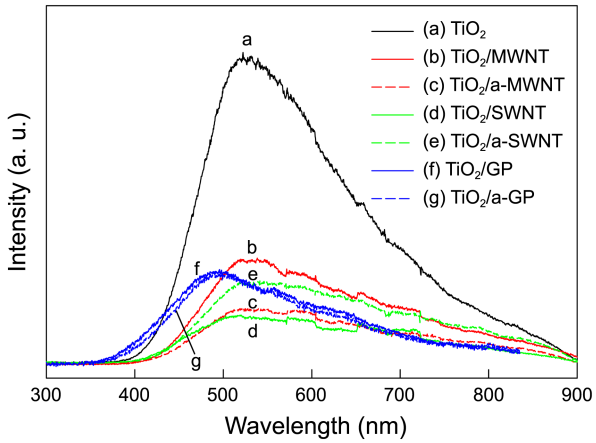

Figure 4. Photoluminescence (PL) emission spectra of bare TiO_2 and TiO_2 composites.

similar band positions (except for GP with blue shift of *ca.* 40 nm due to strong emission by GP itself in the region of 400-500 nm).[58,59] This indicates that the electron-hole recombination is effectively inhibited on the composites likely due to facile and rapid electron transfer from TiO_2 to carbon materials. For such electron transfer, carbon materials should have intrinsically larger work functions than TiO_2 (*i.e.*, more positive energy level than TiO_2 conduction band) and high electron mobility (*i.e.*, electrical conductivity). It was reported that carbon materials have similar work functions with 4.8-5.05 eV,[60] energetically capable of receiving photogenerated electrons from TiO_2 (work function of conduction band *ca.* 4.0 eV). However, the electrical conductivity is significantly different among virgin carbon materials and markedly increases by acid treatment (Table 1).[60,61]

It appears that the H_2 production, electrical conductivity, and PL emission intensity are inter-related because the high electrical conductivity of carbon materials facilitates electron transfers from TiO_2, inhibiting charge recombination (decrease in PL emission intensity) and consequently enhancing H_2 production. However, plots among the three factors fail to display correlation with full data set despite some correlations under limited conditions (Fig. S2). For example, acid treatment increases the electrical conductivities of MWNT, SWNT, and GP by a factor of around 100 (Table 1). Due to this effect, TiO_2/a-MWNT displays reduced PL band and enhanced H_2 production as compared to TiO_2/MWNT. Despite the smaller electrical conductivity of virgin SWNT, however, TiO_2/SWNT shows reduced PL band and is more effective in producing H_2 compared to TiO_2/a-SWNT. GP also displays a unique behavior in that the intensity of PL band is only slightly changed, yet electrical conductivity and H_2 production are significantly enhanced by acid treatment.

Such irrelevancy among the three factors may imply the presence of other hidden factors. Among them, the most probable is the physicochemical coupling state or the stability between TiO_2 and carbon materials. If the coupling is robust and stable without any composite disintegration during photocatalytic reactions, the interparticle charge transfers may be

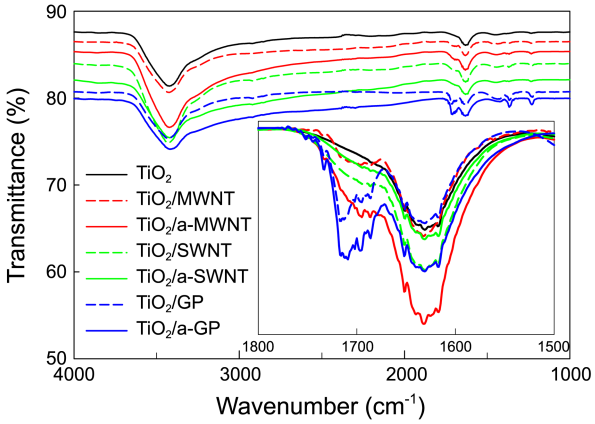

Figure 5. FTIR spectra of bare TiO_2 and TiO_2 composites. Inset shows the magnified spectra of Ti-O-C vibration in the range between 1500 and 1800 cm^{-1}.

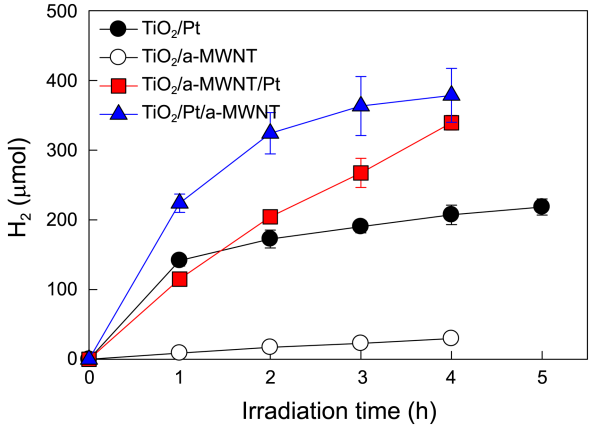

Figure 6. Time-profiled H_2 production in AM 1.5 light-irradiated suspensions of TiO_2 composites with Pt and/or MWNT. Experimental conditions identical to those of Figure 1.

facile and hence the charge recombination should be inhibited. In contrast, if the TiO_2/carbon composites are decoupled or the interparticle interaction is weak, the electron transfer may be limited although neighboring carbon materials have high electrical conductivity. To verify this conjecture, FTIR analysis was carried out for TiO_2 composites with MWNT, SWNT, and GP (Fig. 5). Overall spectra are similar among samples with two apparent IR bands for Ti-OH (3425 cm^{-1}) and Ti-O-C (1635 cm^{-1}).[62,63] Both bands are typically found in TiO_2 samples because of surface titanol groups (Ti-OH) and ubiquitous carbon sources (*e.g.*, CO_2 gas) or carbon impurities adsorbed onto TiO_2. However we note that Ti-O-C bands of TiO_2/MWNT and TiO_2/GP, which display similar intensity to that of bare TiO_2, grow by acid treatment of the respective carbon materials. This strongly suggests that TiO_2 holds a-MWNT and a-GP more tightly than the respective virgin ones. Such tight interconnection should facilitate electron transfer to a-MWNT and a-GP with high electrical conductivity, resulting in a decrease and little change in the PL bands at TiO_2/a-MWNT and TiO_2/a-GP, respectively. As a result, both a-MWNT and a-GP induce positive effects for H_2 production. In contrast, the Ti-O-C band of TiO_2/a-SWNT is weaker than that of TiO_2/SWNT and displays similar intensity to that of bare TiO_2. This also indicates that the interparticle connection between TiO_2 and SWNT becomes weaker by acid treatment. Accordingly, although a-SWNT has higher electrical conductivity, the interparticle electron transfer is limited, the PL band increases, and H_2 production is reduced. This result suggests that although electrical conductivity is essentially important, the physicochemical coupling state of the composites also plays a key role in controlling photocatalytic activity for H_2 production.

Finally, the effect of Pt was compared to a-MWNT in order to examine applicability of a-MWNT as a Pt alternative or Pt-coupled catalyst to TiO_2 photocatalysis (Fig. 6). It was found that TiO_2/Pt exhibits 6-7 fold-higher H_2 production activity than TiO_2/a-MWNT, yet lost its activity after a few hours likely due to Pt fouling. When Pt and a-MWNT are used as a coupled catalyst, the H_2 production is almost doubled. The greater synergic effect of TiO_2/Pt/a-MWNT (a-MWNT deposited on TiO_2/Pt) than TiO_2/a-MWNT/Pt (Pt deposited on TiO_2/a-MWNT) results likely from better charge transfer between TiO_2 and Pt. These synergic effects are practically important because a-MWNT can reduce the use of Pt substantially.

Photocatalytic Oxidation of Organic Substrates. For PCO activity of TiO_2 composites, phenol was selected as a model substrate primarily because of its representativeness as an aquatic pollutant and absence of light screening effect. It was found that only the trace amount of phenol (*ca.* 4%) is adsorbed either on bare TiO_2 and TiO_2/carbon composites. This indicates that 1) carbon materials with large surface areas (particularly AC, CNF, SWNT, and MWNT: see Table 1) actually play a very limited role in binding phenol at circum-neutral pH (pK_a of phenol ~ 10), and hence 2) most PCO reactions of phenol may occurs in Helmholtz double layer region (outer-sphere reaction), not *via* surface-complexation (inner-sphere reaction). Figure 7(a) compares the PCO of phenol, where *ca.* 45% of initial phenol (0.5 mM) is degraded by following a pseudo-first order kinetics in bare TiO_2 ($-k_{obs}$ = 0.013 min^{-1}; $R^2 > 0.99$) (eq. 1).

$$\ln (C_t/C_0) = -k_{obs} \cdot t$$

Only marginal differences (maximum *ca.* 20%) for k_{obs} values (mostly $R^2 \geq 0.99$) are obtained for all TiO_2 composites (Fig. 7(c)). Acid treatment also insignificantly affects the PCO activity of TiO_2 composites (except for a-AC; Fig. 7(b)). Reduced activity of TiO_2/a-AC may be attributed to a change in porosity of AC, an important factor in TiO_2/AC photocatalysis.[64] a-MWNT, which exhibits the highest H_2 production, does not enhance the PCO activity of TiO_2 as well. However, TiO_2/Pt/a-MWNT ternary composite markedly increases k_{obs} value by ~40% (Fig. 7(c)). The intermediate study further shows that hydroquinone and catechol are main intermediates and their time-profiled changes are not much different among carbon materials (virgin and acid-treated) (Fig. S3). This result therefore suggests that 1) although carbon materials have a similar role to Pt in terms

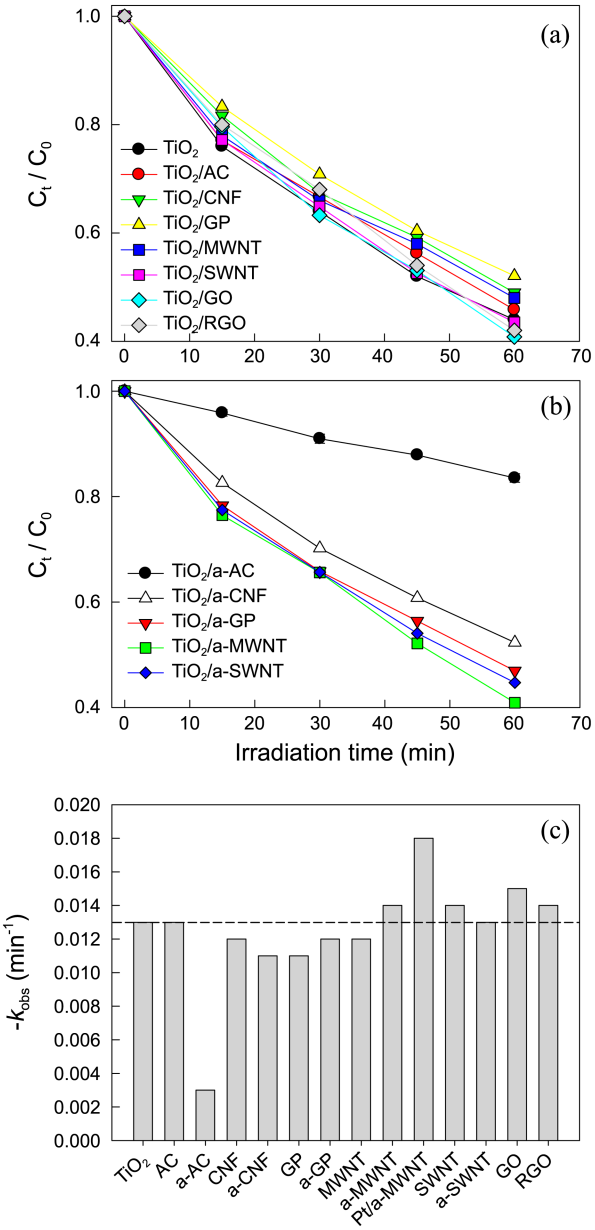

Figure 7. Time-profiled decays of phenol in AM 1.5 light-irradiated suspensions of TiO_2 composites with (a) virgin carbon materials (b) acid-treated carbon materials. (c) shows the relative activity of TiO_2 composites with respect to bare TiO_2 in terms of pseudo-first order kinetics for phenol decay. [catalyst] = 0.5 g/L; $[PhOH]_0$ = 0.5 mM. See Figure 1 for other experimental conditions.

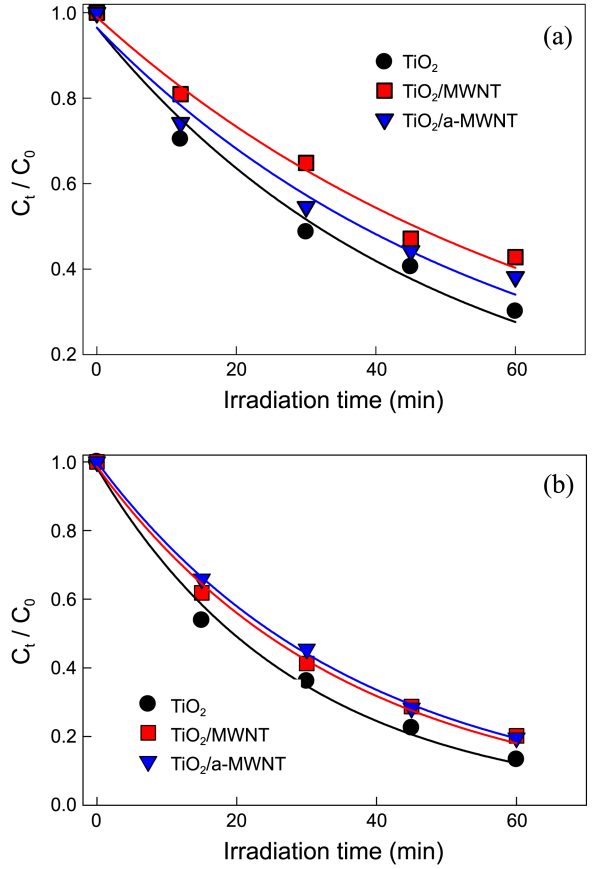

Figure 8. Time-profiled decays of (a) Methylene Blue and (b) Rhodamine-B in AM 1.5 light-irradiated suspensions of TiO_2 composites with MWNT or a-MWNT. [catalyst] = 0.5 g/L; $[MB]_0$ = 0.1 mM; $[Rh\text{-}B]_0$ = 0.2 mM.

of electron reservoir, they play an insignificant role in PCO reaction in contrast to Pt, 2) similarly to H_2 production, co-existence of Pt and carbon materials (a-MWNT) induces a synergy effect, and 3) the degradation mechanism of phenol is not altered by carbon materials. It should be noted that the effect of carbon materials on the PCO of phenol varies and is even contradictory.[35,36,39,40] Such diverse effects suggest that the PCO is very sensitive to ratios of TiO_2 and carbons, preparation method of composites, and surface states.

Instead of phenol, two dye substrates (MB and Rh-B) were also tested with TiO_2/MWNT composites. Indeed, dye substrates are not suitable probe molecules to investigate and evaluate the photocatalytic activities of TiO_2 because they have strong UV-Vis light absorption (light screening effect), easy adsorption on TiO_2 surface, and existence of sensitized degradation mechanism.[65] Nevertheless, most studies on the PCO reactions of TiO_2/carbon composites employed dye substrates as model compounds. It was found that approximately 25% of initial MB (3.3 mmoles/g-TiO_2) is adsorbed to TiO_2 surface in the dark and around 60% of remaining MB (present in bulk solution) is degraded in 1 h-irradiation with $-k_{obs}$ value of ~0.02 min^{-1} (Fig. 8(a)). Meanwhile, TiO_2/MWNT can bind *ca.* 35% of initial MB but exhibits reduced PCO activity for remaining MB with $-k_{obs}$ value of ~0.015 min^{-1}. TiO_2 composites with a-MWNT display a similar behavior with TiO_2/MWNT ($-k_{obs}$ = ~0.017 min^{-1}). In the case of Rh-B, overall behaviors for its adsorption and PCO degradation are not much different from MB with around 0.035, 0.029, and 0.027 min^{-1} (all $R^2 > 0.99$) for the $-k_{obs}$ values of TiO_2, TiO_2/MWNT, and TiO_2/a-MWNT, respectively (Fig. 8(b)).

A few studies reported that UV-irradiated TiO_2/carbon composites generate a larger number of hydroxyl radicals[38,48,52] likely due to effective charge separation and consequently increase in number of available holes. To examine if hydroxyl radicals are produced more in TiO_2/carbon composites, the

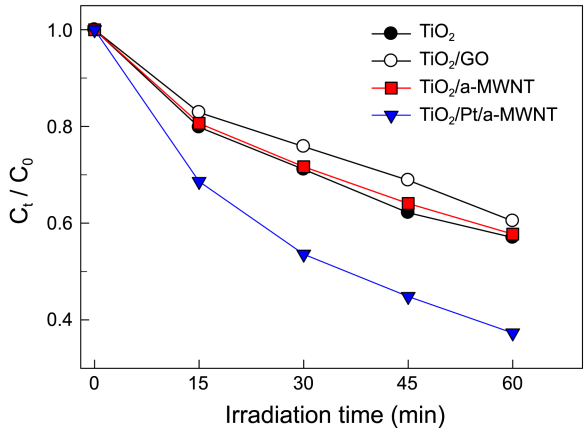

Figure 9. Photocatalytic decay curves of *N,N*-dimethyl-*p*-nitrosoaniline (RNO: an OH radical probe molecule) in AM 1.5 light-irradiated suspensions of TiO_2/carbon composites with or without Pt. [catalyst] = 0.5 g/L; $[RNO]_0$ = 1 mM.

photocatalytic degradation (*i.e.*, transformation) of RNO, OH radical probe molecule,[54,66] was tested. As shown in Figure 9, bare TiO_2, TiO_2/a-MWNT, and TiO_2/GO display very similar decay profile for RNO, whereas TiO_2/Pt/a-MWNT ternary composite displays enhanced RNO decay profile. This result is consistent with the PCO reactions of phenol and dyes in that the effect of carbon materials is insignificant whereas Pt deposition activate the TiO_2/carbon binary composites.

The minor effect of carbon materials may be attributed to various factors. First, hole transport between TiO_2 and substrates can be interrupted due to carbon materials. Large surface areas of carbon materials are beneficial in accumulating substrates inside of carbon materials but such situations also can hinder interaction between substrates and holes. Second, carbon materials can prevent incident photons from reaching TiO_2, and consequently reduce the frequency of photoexcitation (shielding effect). Finally, the intrinsic charge transfer kinetics is also related to the minor effects. It was reported that interfacial electron transfer at TiO_2 is three orders of magnitude slower than hole transfer and considered a rate-determining step in TiO_2 photocatalysis.[2,11,12] In the PCR reaction (H_2 production) occurring in anoxic conditions (N_2-purged), there is virtually no competitive electron acceptor other than proton (H^+). Hence irrespective of the types of carbon materials and physicochemical coupling states of TiO_2/carbon composites, highly electroconductive carbon materials can catalyze the proton reduction (H_2 production) significantly influencing the H_2 production. Conversely, the PCO reactions take place in the presence of dissolved oxygen, a well-known electron quencher. In this oxic condition, hole transfer is relatively less limited by the electron transfer even in bare TiO_2 photocatalysis and thus the effect of carbon materials on the hole transfer may be minor.

Conclusions

This study investigated the effects of carbon materials on the photocatalytic redox reactions of TiO_2. A series of TiO_2 and carbon material composites were successfully prepared by an evaporation method. The composites show apparent synergetic effects for photocatalytic H_2 production yet with varying degrees due to the different electrical conductivities of carbon materials, charge recombination behaviors of TiO_2/carbon composites, and the physicochemical coupling states between TiO_2 and carbon materials. Acid treatment of carbon materials changes theses parameters, resulting in significantly different photocatalytic activities. Meanwhile, carbon effects are found less apparent for the kinetics and mechanisms in photocatalytic oxidation reactions of TiO_2 for all tested substrates. Such markedly different effects of carbon materials on TiO_2 photocatalysis are partly attributed to intrinsic charge transfer kinetics. However, when Pt is coupled to TiO_2/carbon binary composites, such kinetic limits vanish and photocatalytic activity is maximized. These results are very important and informative in designing high efficiency photocatalysis of TiO_2/carbon composites.

Acknowledgments. This research was supported by the Basic Science Research Program (No. 2012R1A2A2A01004517) and the Human Resource Training Project for Regional Innovation (2012H1B8A2026280) through the National Research Foundation of Korea (NRF) funded by the Ministry of Education, Science, and Technology, and by Kyungpook National University Fund, 2012.

References

1. Chen, X.; Shen, S.; Guo, L.; Mao, S. S. *Chem. Rev.* **2010**, *110*, 6503.
2. Hoffmann, M. R.; Martin, S. T.; Choi, W.; Bahnemann, D. W. *Chem. Rev.* **1995**, *95*, 69.
3. Park, H.; Vecitis, C. D.; Choi, W.; Weres, O.; Hoffmann, M. R. *J. Phys. Chem. C* **2008**, *112*, 885.
4. Park, H.; Vecitis, C. D.; Hoffmann, M. R. *J. Phys. Chem. A* **2008**, *112*, 7616.
5. Asahi, R.; Morikawa, T.; Ohwaki, T.; Aoki, K.; Taga, Y. *Science* **2001**, *293*, 269.
6. Khan, S. U. M.; Al-Shahry, M.; Ingler, J. W. B. *Science* **2002**, *297*, 2243.
7. Park, Y.; Kim, W.; Park, H.; Tachikawa, T.; Majima, T.; Choi, W. *Appl. Catal. B* **2009**, *91*, 355.
8. Youngblood, W. J.; Lee, S.-H. A.; Maeda, K.; Mallouk, T. E. *Accounts Chem. Res.* **2009**, *42*, 1966.
9. Park, H.; Choi, W. *Langmuir* **2006**, *22*, 2906.
10. Park, H.; Bae, E.; Lee, J.-J.; Park, J.; Choi, W. *J. Phys. Chem. B* **2006**, *110*, 8740.
11. Park, H.; Choi, W. *J. Phys. Chem. B* **2004**, *108*, 4086.
12. Park, H.; Choi, W.; Hoffmann, M. R. *J. Mater. Chem.* **2008**, *18*, 2379.
13. Serp, P.; Figueiredo, J. L. *Carbon Materials for Fatalysis*; John Wiley & Sons: New Jersey, 2009.
14. Dillon, A. C. *Chem. Rev.* **2010**, *110*, 6856.
15. Guldi, D. M.; Sgobba, V. *Chem. Commun.* **2011**, *47*, 606.
16. Leary, R.; Westwood, A. *Carbon* **2011**, *49*(3), 741.
17. Zhang, L.-W.; Fu, H.-B.; Zhu, Y.-F. *Adv. Func. Mater.* **2008**, *18*(15), 2180.
18. Gao, B.; Peng, C.; Chen, G. Z.; Puma, G. L. *Appl. Catal. B* **2008**, *85*(1-2), 17.
19. Li, Z.; Gao, B.; Chen, G. Z.; Mokaya, R.; Sotiropoulos, S.; Puma,

G. L. *Appl. Catal. B* **2011**, *110*, 50.
20. Jiang, G.; Lin, Z.; Zhu, L.; Ding, Y.; Tang, H. *Carbon* **2010**, *48*(12), 3369.
21. Yu, J.; Ma, T.; Liu, G.; Cheng, B. *Dalton T.* **2011**, *40*(25), 6635.
22. Yang, Y.; Qu, L.; Dai, L.; Kang, T.-S.; Durstock, M. *Adv. Mater.* **2007**, *19*(9), 1239.
23. Ahmmad, B.; Kusumoto, Y.; Somekawa, S.; Ikeda, M. *Catal. Commun.* **2008**, *9*(6), 1410.
24. Kongkanand, A.; Kamat, P. V. *ACS Nano* **2007**, *1*(1), 13.
25. Kongkanand, A.; Kamat, P. V. *Nano Lett.* **2007**, *7*(3), 676.
26. Park, Y.; Kang, S.-H.; Choi, W. *Phys. Chem. Chem. Phys.* **2011**, *13*(20), 9425.
27. Ng, Y. H.; Lightcap, I. V.; Goodwin, K.; Matsumura, M.; Kamat, P. V. *J. Phys. Chem. Lett.* **2010**, *1*, 2222.
28. Lightcap, I. V.; Kosel, T. H.; Kamat, P. V. *Nano Lett.* **2010**, *10*(2), 577.
29. Bell, N. J.; Ng, Y. H.; Du, A.; Coster, H.; Smith, S. C.; Amal, R. *J. Phys. Chem. C* **2011**, *115*, 6004.
30. Zhang, W. L.; Choi, H. J. *Chem. Commun.* **2011**, *47*(45), 12286.
31. Zhang, X.-Y.; Li, H.-P.; Cui, X.-L.; Lin, Y. *J. Mater. Chem.* **2010**, *20*(14), 2801.
32. Xiang, Q.; Yu, J.; Jaroniec, M. *Nanoscale* **2011**, *3*(9), 3670.
33. Fan, W.; Lai, Q.; Zhang, Q.; Wang, Y. *J. Phys. Chem. C* **2011**, *115*(21), 10694.
34. Kim, H. C.; Moon, G.; Monllor-Satoca, D.; Park, Y.; Choi, W. *J. Phys. Chem. C* **2012**, *116*, 1535.
35. Colon, G.; Hidalgo, M. C.; Macias, M.; Navio, J. A. *Appl. Catal. A* **2004**, *259*(2), 235.
36. El-Sheikh, A. H.; Al-Degs, Y. S.; Newman, A. P.; Lynch, D. E. *Sep. Purif. Technol.* **2007**, *54*(1), 117.
37. Torimoto, T.; Okawa, Y.; Takeda, N.; Yoneyama, H. *J. Photochem. Photobiol. A* **1997**, *103*(1-2), 153.
38. Yu, Y.; Yu, J. C.; Chan, C. Y.; Che, Y. K.; Zhao, J. C.; Ding, L.; Ge, W. K.; Wong, P. K. *Appl. Catal. B* **2005**, *61*(1-2), 1.
39. Wang, W. D.; Serp, P.; Kalck, P.; Faria, J. L. *Appl. Catal. B* **2005**, *56*(4), 305.
40. Vajda, K.; Mogyorosi, K.; Nemeth, Z.; Hernadi, K.; Forro, L.; Magrez, A.; Dombi, A. *Phys. Status Solidi B* **2011**, *248*(11), 2496.
41. Woan, K.; Pyrgiotakis, G.; Sigmund, W. *Adv. Mater.* **2009**, *21*(21), 2233.
42. Jafry, H. R.; Liga, M. V.; Li, Q.; Barron, A. R. *New J. Chem.* **2011**, *35*(2), 400.
43. Dechakiatkrai, C.; Chen, J.; Lynam, C.; Phanichphant, S.; Wallace, G. G. *J. Electrochem. Soc.* **2007**, *154*(5), A407.
44. Yao, Y.; Li, G.; Ciston, S.; Lueptow, R. M.; Gray, K. A. *Environ. Sci. Technol.* **2008**, *42*(13), 4952.
45. Kim, S.; Lim, S. K. *Appl. Catal. B* **2008**, *84*(1-2), 16.
46. Modestov, A.; Glezer, V.; Marjasin, I.; Lev, O. *J. Phys. Chem. B* **1997**, *101*, 4623.
47. Zhang, H.; Lv, X.; Li, Y.; Wang, Y.; Li, J. *ACS Nano* **2010**, *4*(1), 380.
48. Zhang, Y.; Tang, Z.-R.; Fu, X.; Xu, Y.-J. *ACS Nano* **2010**, *4*(12), 7303.
49. Akhavan, O.; Abdolahad, M.; Esfandiar, A.; Mohatashamifar, M. *J. Phys. Chem. C* **2010**, *114*, 12955.
50. Mao, C.-C.; Weng, H.-S. *Chem. Eng. J.* **2009**, *155*(3), 744.
51. Oh, W.-C.; Jung, A.-R.; Ko, W.-B. *Mater. Sci. Eng. C* **2009**, *29*(4), 1338.
52. Zhang, Y.; Tang, Z.-R.; Fu, X.; Xu, Y.-J. *ACS Nano* **2011**, *5*(9), 7426.
53. Hummers, W. S.; Offeman, R. E. *J. Am. Chem. Soc.* **1958**, *80*, 1339.
54. Yang, S. Y.; Choo, Y. S.; Kim, S.; Lim, S. K.; Lee, J.; Park, H. *Appl. Catal. B* **2012**, *111-112*, 317.
55. Ou, Y.; Lin, J.; Fang, S.; Liao, D. *Chem. Phys. Lett.* **2006**, *429*(1-3), 199.
56. Dai, K.; Peng, T.; Ke, D.; Wei, B. *Nanotechnology* **2009**, *20*(12), 125603.
57. Choi, S. K.; Kim, S.; Lim, S. K.; Park, H. *J. Phys. Chem. C* **2010**, *114*, 16475.
58. Zhou, K.; Zhu, Y. F.; Yang, X.; Jiang, X.; Li, C. *New J. Chem.* **2011**, *35*, 353.
59. Chang, S.-S. *Mater. Sci. Eng. B* **2004**, *B106*, 56.
60. Kim, Y.; Park, H. *Energy Environ. Sci.* **2011**, *4*, 685.
61. Kim, Y.; Park, H. *Appl. Catal. B* **2012**, *125*, 530.
62. Atik, M.; Zarzycki, J. *J. Mater. Sci. Lett.* **1994**, *13*, 1301.
63. Sener, S.; Erdemoglu, M.; Asilturk, M.; Sayilkan, H. *Turk. J. Chem.* **2005**, *29*, 487.
64. Velasco, L. F.; Parra, J. B.; Ania, C. O. *Appl. Surf. Sci.* **2010**, *256*(17), 5254.
65. Ohtani, B. *Chem. Lett.* **2008**, *37*, 217.
66. Comninellis, C. *Electrochim. Acta* **1994**, *39*, 1857.